Technical Report RSC-33

QUANTITATIVE EVALUATION OF WATER QUALITY IN THE COASTAL ZONE BY REMOTE SENSING

by

WESLEY P. JAMES
Environmental Engineering Division
Department of Civil Engineering

September 1971

supported by
National Aeronautics and Space Administration
NASA Grant NsG 239-62
and
Texas Water Quality Board
IAC (72-73) – 156

NRL 44-001-601

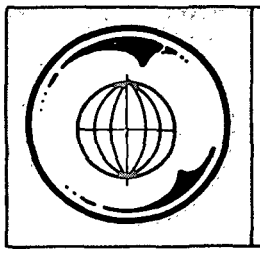

TEXAS A&M UNIVERSITY
REMOTE SENSING CENTER
COLLEGE STATION, TEXAS

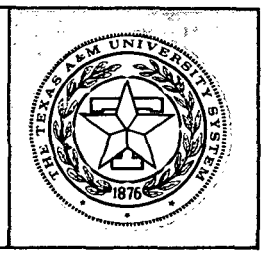

Technical Report RSC-33

QUANTITATIVE EVALUATION OF WATER QUALITY IN THE COASTAL ZONE BY REMOTE SENSING

by

WESLEY P. JAMES
Environmental Engineering Division
Department of Civil Engineering

September 1971

supported by

National Aeronautics and Space Administration

NASA Grant NsG 239-62

and

Texas Water Quality Board

IAC (72-73)-156

TABLE OF CONTENTS

LIST OF FIGURES

Technical Report RSC-33

QUANTITATIVE EVALUATION OF WATER QUALITY IN THE COASTAL ZONE BY REMOTE SENSING

by

W. P. James

Estuaries in the coastal zone are a valuable resource. Urban centers along the coast are increasing in size and are creating environmental quality stresses. The ocean has been and will continue to receive much of man's waste material. The sea, however, does not have an unlimited ability assimilate waste, but it has a finite capacity. Even this capacity can not be fully utilized since the limiting factors will be localized problems created by population centers and compounded by the limited mixing and circulation characteristics of the estuaries and near shore waters.

The purpose of a waste management program is to maintain the environmental quality at an acceptable level at a minimum cost. Such a program requires that decisions be made which alter the present methods of waste disposal. These decisions can not effectively be made without a better understanding of the relationships that exist between the various components of the coastal area. In situ sampling methods for point measure-

ments of water pollution is not adequate for monitoring a large aquatic system.

Remote sensing offers the possibility of providing a comprehensive understanding of the coastal area and providing quantitative data on the response of the system to pollutants. Environmental quality monitoring will provide the feedback loop to show the relationship between waste management decisions and the environmental quality.

THE ESTUARY

The estuary is a mixing basin where the ocean water and fresh water streams meet. It is characterized by extremes in temperature, salinity, water quality, currents and bottom deposits. In addition, the intertidal zone is subjected to alternate exposure to air and water. This complex ecological system is often the most biologically variable and the most productive area in the marine environment. Besides its permanent inhabitants, it also serves as a nursery ground for many forms of life.

The flora and fauna must survive extreme hydrographis changes in a wide variation of turbidity, temperature and salinity. Some animals have become adapted to

the extremes in the estuary, but often faunal populations are destroyed. Plankton generally remain in the slower moving parts of the estuary long enough to develop populations. The diagram in Figure 1 shows some of the complex relationships in the estuarine environment.

About 3000 years ago the sea attained its present level and in a few more thousand years estuaries may be quite rare. The relative length of an estuary's life is determined primarily by the rate at which sediments are introduced and deposited in it. Where large volumes of sediments are introduced by streams, the estuary will be short-lived.

Soil sediments are transported into the system by the ocean, wind, and streams. Erosion by wave action and currents combined with selective settlementation modify the bottom deposits within the estuary. Active sand dunes are present along the lower reaches of many estuaries and can provide a source of poorly-graded, sandy material. The bay entrance forms a natural sediment trap for the littoral drift along the coast. The trapped material is carried into the bay on flood tide. The ebb tide removes material from the system. Near the head of the estuary soil deposits tend to be silt and clay size of fluvial origin. Advancing deltas from

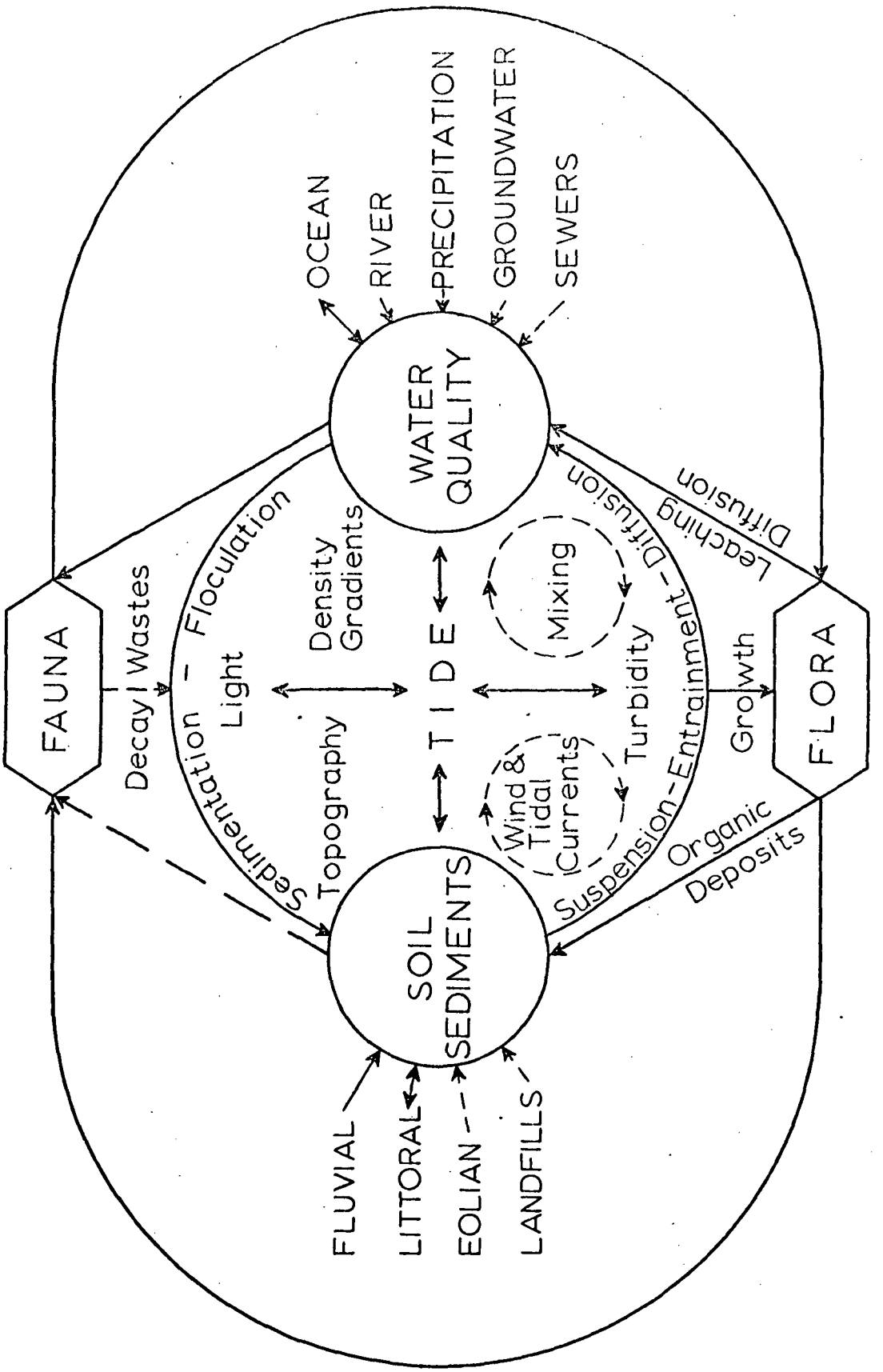

Figure 1. The estuarine system.

streams are a natural enemy of the estuary. The current velocity in the estuary is likely to be small and turbulence insufficient to transport the suspended material through the system.

The soil deposits in the embayment tend to be predominantly sand of littoral origin near the mouth and fine grain material of fluvial origin near the head. The particle size of the deposits depend upon the origin of the material and the current velocity. Vegetation also influences the character of the deposits. As rooted plants begin colonization of the tidal flat, the cover aids in trapping fine sediments. The increase in sediment deposits raise the elevation of the tidal flat. When the area is covered by only a few inches of water at normal high tide, a marsh is likely to be formed. The tidal flats can change from sand flats in the lower reaches, mud flats in the middle reach, marsh in the upper reach and pasture land near the head of the estuary.

The primary sources of water in most estuaries are the ocean and fresh water streams. The ocean water with relatively constant characteristics provides a buffer in the system. In the lower reaches of the estuary, the change in oxygen, temperature and salinity tend to be small. The fresh water inflow at the head

of the estuary generally varies greatly. The salinity at the head of the estuary may be greater than that of the sea during periods of low river flow and high evaporation and approach zero during periods of high inflow. Temperature of the fresh water inflow also has a large seasonal variation.

The major factors that determine the mixing characteristics in the estuary are the wind, tidal range, topography, fresh water inflow and salinity gradients. The salinity or density gradients are functions of the fresh and salt water inflow and the circulation within the estuary. Energy must be provided to break down these gradients to allow complete mixing.

Temperature, oxygen and nutrient concentrations are important water quality characteristics. Due to higher water temperatures, the critical time for pollution will normally occur in late summer or early fall. The higher temperature decreases oxygen solubility and increases the rate of biochemical oxidation. Factors affecting the oxygen content include depletion due to biological degradation, oxygen provided by physical reaeration and photosynthesis, and oxygen content of the estuary influent and effluent. The ocean waters are usually at saturation due to the wind turbulence

and provide a valuable source of oxygen for the estuary. Diurnal variations in oxygen concentrations are found in many parts of the estuary. The most important nutrient compounds are those which yield phosphate phosphorus and nitrate nitrogen. These compounds are necessary to the metabolism of most aquatic forms and their presence or absence plays a major role in determining the size of the biological population present. Most ocean water has very low concentrations of these nutrients, and as a result the salt water entering an estuary may be nutrient deficient.

Nutrients are added to an estuary by freshwater inflow and waste discharges as well as through the influx of salt water. The nutrient concentration of freshwater streams is extremely variable. In most unpolluted streams however, a nutrient deficiency is common. The major sources of nutrients in fresh water are normally drainage from agricultural lands and effluents from sewage treatment plants. The effluent from a secondary sewage treatment plant may be considerably higher in nitrates that the freshwater supply. The increase in nutrient levels stimulate biological growth and increase the oxidation rate of organic pollutants. The increased oxygen demand can depress the oxygen concentration to dangerously low levels.

The great bulk of the organic material in the estuary is derived from vegetation. The amount of material entering the system is related to seasonal decay cycle of the vegetative cover of the watershed. Only a small portion of the production of marsh grass is grazed while it is alive. Much of this material is returned to the estuary by the detritus food chain. The plant detritus which tends to persist longest includes structural material composed mainly of cellulose and lignins. While some nutrients become available immediately for the consumer, the bulk of the plant material may require months for decomposition. Wave and water current turbulences reduce the size of the organic material. The reduction in particle size increases the rate of chemical simplification by hydrolysis and oxidation.

Rivers entering the estuary carry negative charged organic particles. Some of these particles are precipitated by positively charged metallic ions of the salt water. Positively charged organic particles may persist for sometime suspended in the water. Colloidal organic micelles tend to adhere to exposed surfaces forming oozes and slimes on surfaces and organic sludges on the bottom. Organic material is stored in the estuarine system as suspended, colloids or molecules in the

water, in the bodies of living plants and animals and in the bottom deposits. Water turbulence that entrains bottom deposits changes the supply of available food and affects the water quality.

Plant life in the estuary include phytoplankton, marginal submerged vegetation and mud flat diatons and filamentous algae. Algae evolve oxygen during their growth but remove oxygen from the system in the absence of sunlight. Large populations can create large diurnal variations in oxygen concentration. The turbidity causing attenuation of light limits the growth of the rooted vegetation and algae. Saprophytic bacteria are associated with organic material and serve to convert organic matter from a relatively unavailable to relatively available food supply. A few bacteria are capable of photosynthesis and oxidize hydrogen sulfide.

Within the littoral zone are generally various benthic plants grouped according to the depth of the water. Emergent rooted vegetation such as cattails, provide food and shelter for amphibious animals. Raw material for plant growth is obtained from below the water surface. Rooted aquatic plants with floating leaves and submergent vegetation may also be present in the deeper waters. The growth, vigor and expansion

of the various groups of fixed aquatic vegetation will be influenced by the water quality of the area and changes or fluctuations in the water quality parameters. Thus, subtile changes in the water quality created for example by a new waste discharge source might be detected by changes in the aquatic vegetation.

WATER QUALITY

Color and turbidity are perhaps the most obvious water quality parameters to be quantitatively measured by remote sensing techniques. Both may be caused by a variety of materials ranging in size from colloidal to coarse dispersions. Color can be classified as either true or apparent depending on whether it is caused by colloidal or suspended matter. True color generally results from contact of the water with organic debris. Tannins, humic acid, and humates from the decomposition of liginins are considered to be the principal coloring bodies. Surface waters may also become colored by pollution with highly colored waste waters such as those from dyeing operations in the textile industry, from pulping operations in the paper industry and from beet processing in the canning industry. True

color per se is not considered harmful but may cause the water to be aesthetically unacceptable for human use.

Turbidity is a measure of light scatter within the water volume. It is not only aesthetically undesirable but also makes treatment expensive and disinfection difficult for water supply. In the natural environment, the suspended material increases the light attenuation and reduces the amount of light available to the aquatic life. The suspended material will eventually settle out and the sediment can cause serious damage to the marine biota.

Rivers on their way to the sea pick up both organic and inorganic suspended material. Soil erosion from farming, mining, and construction operations are principal sources of turbidity. Turbulance in shallow estuaries and dredging will entrain bottom sediments. Water currents are an important factor in determining the areas affected by the suspended material. Effective treatment of low concentration, large volume waste such as agricultural runoff or storm waste drainage from developed areas is difficult to achieve. Rather that treatment, the solution will be to identify the source and to reduce the volume by proper management techniques.

Organic materials in the water serve as food for the plants and animals. The bacterial and algae growth produce additional turbidity. Plankton occupy a key role in the aquatic food chain. Under proper conditions algae growth can be excessive and can create large diurnal variations in dissolved oxygen. While a certain amount of organic wastes are necessary for the normal biological cycle, too many wastes can destroy it. As the organic concentration increases, the demand for oxygen also increases. In the absence of dissolved oxygen bacteria undergo anaerobic metabolism with its resultant odors and black colors.

The highly reflective characteristics in the near infrared band of the chlorophyll-bearing algae will generally permit detection by remote sensing techniques. The intensity of the signal returned from the water will depend on the concentration and vertical distribution of the plankton. A surface scum will reflect more radiation than a uniform mixture in the water column. Both nitrogen and phosphorus are essential for the growth of phytoplankton. Limitation of these elements will usually control the rate of growth. The critical level for phosphorus has been established near 0.01 mg/1.

In a low organic content estuary, the total number of micro organisms will be low since food is

limiting. A few species of a large number of micro organisms characterize a polluted body of water, while a few micro organisms of a large number of species characterize a non-pulluted body of water. Thus, the number and rate of growth of micro organisms are important water quality parameters and can be a more reliable indicator of pollution than some chemical tests. Dispersed micro organisms predominate in most pollution problems, whereas fixed micro organisms exert a dominant influence only in very shallow waters.

The radiation falling on the particles within the water volume may be reflected or refracted at the particle surface. Radiation that is refracted may be absorbed or transmitted through the particle. Both the surface and internal optical properties of the particles may be selective with respect to the wavelength of the radiation. Under calm water conditions, a high light attenuation rate in the water will cause a higher surface water temperature. Turbulance will tend to cause the surface water temperature to be lower and the temperature to be nearly uniform from the surface to the lower limit of the mixing zone. The variations in temperature of the water will effect the natural balance of the ecosystem. Increased temperature reduces the

dissolved oxygen saturation level and increases rate of biological oxygen demand.

In the calm protected arms of the estuary, the turbulance is low and the surface water is not being mixed with the subsurface waters. The oxygen content can be near saturation at the surface, while anaerobic conditions exist near the bottom. It is in these regions where the most serious water quality problems are likely to occur.

REVIEW

Both the color of the waste and the amount of light scattered from below the water surface can be recorded on aerial photography. Most black and white film used today for aerial photography is panchromatic film which is sensitive to the 400-700 mm region of the spectrum. By using lens filters on the camera, the exposure can be limited to a selected region of the spectrum. Generally the film-filter combination is selected to give maximum contrast between the object and background.

Blue light with a wave length of about 480 nm has the greatest penetration in the deep ocean waters.

In the turbid coastal waters the greatest penetration generally occurs at about 530 nm (Jerlov, 1968). As the composition, size or concentration of particles in the water vary, the band of greatest penetration and color of the sea may also change. Photography can, under certain conditions, be used to distinguish water masses, to delineate current patterns, to identify upwelled water along the coast and to track river plumes in the ocean.

Color photography divides the visible spectrum into three bands. The composition of the light is recorded as blue, green, and red colors on a positive transparency or print. For many applications of aerial photography the three bands are adequate. However, the color film has been designed to reproduce a natural land scene which is visually similar to the original view. The film may not give the best results possible if it is used for other than its designed purpose. Stranberg (1966, 1967) of Itek Data Analysis Center has published numerous examples of color photography for water quality analysis.

Color infrared film is sometimes called false color film. The blue, green and red colors on the photograph result from exposures to the green, red and

infrared bands of the spectrum, respectively (Fritz, 1967). Besides military uses, the film has been used extensively in the detection of disease and insect pests in forest and agriculture crops. It also has been used advantageously in geological and soils interpretation. When using this film, a yellow filter is needed to eliminate the blue light, thereby reducing the degrading effect of haze. As skylight reflection on the water surface is also predominantly blue, infrared color photography of underwater details will appear clearer than with ordinary color photography. Generally, the infrared layer on the film is underexposed when photographing a water body.

Narrow band filters permit the selection of the region of the spectrum that has minimum interference and maximum subject contrast. Interference filters have several advantages over absorption filters including high peak transmittance and sharp cutoffs. However, the peak wavelength of an interference filter is a function of the angle of incidence of the radiation impinging on the filter. If it is desired to record essentially the same band or region of the spectrum on the edges of the frame as in the center of the picture, interference filters should only be used with cameras having a narrow angle

field of view. The same film-narrow band filter combinations used to study one waste can probably not be used to study a different waste.

Multiband camera systems have been developed by several organizations (Yost and Wenderoth, 1967; Molineux, 1965). This system has a number of film-filter combinations to take simultaneous photographs in several regions in the spectrum. This method not only allows the selection of several film-filter combinations for optimum results, but permits the proper exposure of each spectral band. For an example, on a normal color photograph of the sea, the blue sensitive layer is generally over exposed while the red sensitive is generally underexposed. A multiband camera system would allow the proper exposure of each band.

In research at the Allen Hancock Foundation it was found that high optical absorbance of millipore-filtered water to light at a wavelength of 230 nm is related to the concentration of sewage. In their study (Allen ..., 1964) the ultraviolet absorbance was suggested as a possible method of tracing the sewage field by direct sampling without using a tracer. A film sensitive to the ultraviolet region of the spectrum might be used to trace the sewage field. However, the ultra-

violet is also the region of maximum atmospheric interference.

Infrared film is sensitive to both the blue and infrared regions of the spectrum. It is, therefore, necessary to use lens filters in order to limit the exposure to the infrared region. Infrared photography will record energy in the 700-900 nm region. At normal temperatures the energy in this region is predominately reflected energy, not emitted energy, and is not related to temperature. Due to the high attenuation of water in the infrared band, water surfaces on an infrared black and white photograph will normally appear black. The high contrast between the water and land is used to advantage when mapping the water line of a body of water. Algae have high reflectance in this band and infrared photography is used to monitor blooms.

Objects at normal temperature radiate thermal infrared rays at a wavelength greater than can be recorded on ordinary infrared film. Suitable equipment is now available for measuring surface water temperatures by remote sensing. Infrared scanning of 4.5 - 5.5 micron wavelength has been used successfully by the U. S. Geological Survey to locate fresh water springs in Hawaii (Fisher, Davis, and Sousa, 1966). In this study the

sea water temperature averaged 73.5 degrees F while the fresh water temperature was between 60 and 70 degrees F. Scanning in the 8-14 micron wavelength would be most suitable for water surface temperatures as this is the region of maximum radiation and the region relatively free of reflected sunlight interference. It is expected that temperature differences of 0.2 degrees C can be detected by scanning in this region (Ory, 1965). The temperature of the waste may provide a suitable tracer for a thermal effluent discharge. For cooler industrial wastes the use of heat as a tracer is unlikely since the thermal resolution of the scanning equipment is about the same magnitude as the expected maximum difference in temperature within the waste field. In the ocean, vertical thermal stratification will exist under certain conditions. Warm wastes discharged from the diffuser of an ocean outfall will mix with the colder subsurface water and by the time the mixture reaches the surface, the resulting plume temperature may be greater than, less than, or equal to the surrounding ocean temperature.

Scherz (1967) at the University of Wisconsin conducted laboratory tests of various wastes with a reflecting spectrophotometer and aerial photographs of pollution sources. Several of the conclusions from the study are listed as follows:

(1) Normal uncolored salts such as NaCl, Na_2SO_4, and $Na_2PO_4H_2O$ caused no change in the reflection characteristics for distilled water in the photographic range.

(2) Dissolved gases, such as oxygen, and nitrogen caused no appreciable change in the reflection curves of distilled water.

(3) Heat effects of distilled water and lake water cause slight effects in the blue and green areas but none that would show up on a photograph. When the temperature is below 63 degrees C, there is no appreciable change in the reflection characteristics in the infrared region due to temperature effects. When the temperature is raised to above 63 degrees C, there is an increase in reflection in the infrared region that could perhaps be photographed. Temperature this high are not normally encountered in field conditions and one must conclude that normal differences in temperatures in water masses will not show up differently on photographic images due to the temperature effects alone.

(4) Reflection characteristics of waters from lakes and streams vary a great deal. The characteristic curves in many cases are due to suspended matter, and in certain cases to the inherent color of the water.

(5) Various wastes have characteristic reflection curves that are often quite different than those of the receiving water bodies. By analyzing the characteristic curves of the wastes and the receiving waters, one can see where the curves mismatch and

predict how the various liquids will appear on a photographic image. All wastes analyzed in both the laboratory and field could be detected on aerial photography.

Ichiye and Plutchak (1966) of Columbia University took aerial photography of Rhodamine B dye patches and found that the dye concentrations as measured with a ship-borne turner fluorormetric correlated very well with the densitometer headings from the aerial negative.

Cornell Aeronautical Laboratory (Neumaier, 1967; Silvestro, 1969; Piech, 1971) has conducted a number of laboratory and field tests using aerial photographic techniques for water quality analysis. Early phases of the study under project Aqua-Map were conducted similar to those by Scherz. This work was continued to include quantitative evaluation of water quality from aerial photography with test panels submerged below the water surface. Later densitometer traces from an aerial photograph were made across a waste discharge plume in a river and related to the light returned from the waste field through the use of ground test panels. Recent work has been devoted towards eliminating the ground test panels by standardization with natural objects of known reflectance and shadow areas within the scene.

Work by James and Burgess (1969, 1970, 1971) has been devoted to open coastal waters. Unique features of these studies include:

(1) Oblique camera mounting to avoid direct sunlight reflection and to provide shore control within the photos.

(2) Computer processing techniques to rectify the photos, convert densitometer readings to light values, reduce the effects of interferences and compute waste concentrations.

In this work the open sea was used for background standardization of the aerial photography. The ratio of light returned in two bands was related to the waste concentration in an ocean outfall waste plume. For approximately 10 sampling runs, the correlation coefficient between the boat sampling and the aerial photography with about 200 degrees of freedom ranged from 0.85 to 0.95. Several of the conclusions of this study were:

(1) Aerial photography provides an effective method for a comprehensive analyses of the dispersion of wastes that are discharged into the ocean.

(2) Aerial photographs showing the transport and spread of dye patches will provide detailed designed information for evaluating proposed ocean outfall sites throughout the year.

(3) Characteristic airphoto pattern elements can be utilized to estimate wind velocity, sea state, and diffusion coefficients in the coastal waters.

(4) In addition to being technically feasible, aerial photography was shown to be an economically feasible method for acquiring ocean outfall data prior to construction.

QUANTITATIVE EVALUATION

Quantitative evaluation of water quality requires that computations be made regarding location, area affected and the magnitude of parameters. The major advantage of remote sensing is that it can cover a large area in a short time. The resulting large volume of data will generally require computer processing. If aerial photography is used as the sensor to collect the data, the photographic imagery must be converted to digital information through the use of a photo densitometer. Multispectral scanners record the information from several bands directly on magnetic tape and save this additional processing step.

The presence of thermal pollution can best be detected by an infrared line scanner. Scanners sensitive to the 8 to 14 micron region of the spectrum can detect temperature differences as small as 0.2°C. Surface water temperature distributions can be mapped, and in many cases

water masses identified by their temperature and their boundaries delineated. Thus the area of influence of thermal discharges cna be determined. Since the instrument measured emitted radiation rather than reflected sunlight, operations are not limited to daylight hours.

Photographic films and most multispectral scanners used in remote sensing of water quality are sensitive to some portion of the visible or near visible light. The main source of this light is the sun. Both the intensity and composition of the light scattered from within the water can be measured and in many cases related to certain water quality parameters. With the multispectral scanners the strength of the returned signal in the various bands indicates the brightness and color of the scattered light. The amount of light is recorded with aerial photography as the film density of the photographic image while the composition is determined from the film-filter combinations. If there are many photographic bands, the volume of film to handle can become large and the data processing may become involved.

If the light scattering or light absorbing property of the water is a function of wavelength of light the ratio of the light returned in the band of

maximum scatter to the light return in the band of maximum absorption should be a sensitive indicator of the water quality parameter. However, if the material within the water causes it to appear black, white or some shade of gray, the sum of the light returned in two bands divided by their difference may provide a sensitive indicator of the material. The purpose of using the ratio of light returned in two bands is that several unknown factors are cancelled from both the numerator and denominator of the equation, simplifying the relationship with the water quality parameter.

Factors which may interfer with the quantitative evaluation of water quality include the contrast attenuation in the atmosphere due to light path radiance, reflections from the water surface and light reflected from the bottom of the water body. Light scatter in the atmosphere provides valuable information in air quality studies. The reflections from the water surface can be utilized to study water roughness and for analyzing films on the water surface. The composition of the signal returned from the bottom can provide information on soil sediments and aquatic vegetation. The effects of these factors can be changed by data acquisition and processing techniques depending on the

purpose of the survey. The following sections give the rationale for quantitative evaluation of the water quality.

Sun Energy

Energy from the sun passes through the atmosphere to the sea. Upon reaching the water surface, the radiation is either reflected or transmitted through this interface. The refracted light is transmitted, scattered, or absorbed in the sea. Some of the scattered light is directed upwards and passes through she sea-air interface. A part of the light emerging from the sea reaches the sensor and is recorded.

The upper limit of the atmosphere receives energy at an average rate of about 0.135 watts per square cm perpendicular to the radiation. This value fluctuates about ±5% during a yearly period due to the eccentricity of the earth's orbit about the sun. The extraterrestrial energy spectrum of the sun's radiation is shown in Figure 2 (Hutchinson, 1957).

The normal spectrum of solar radiation that reaches the sea surface is also shown in Figure 2. Solar radiation, when passing through the atmosphere, is reduced by scattering and absorption. The amount of radiation re-

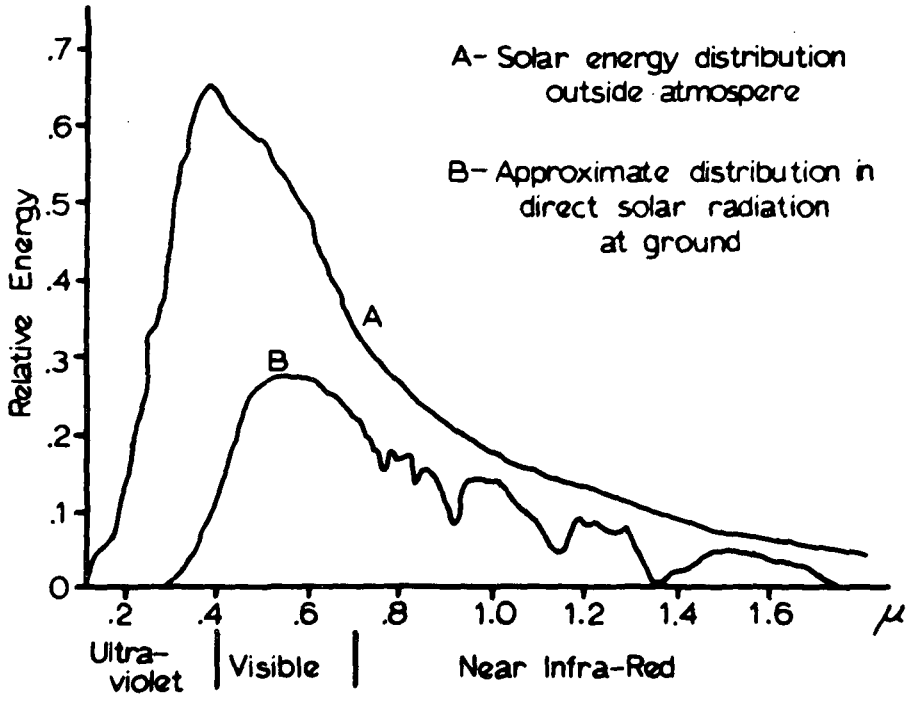

Figure 2. Spectral distribution of radiant energy.

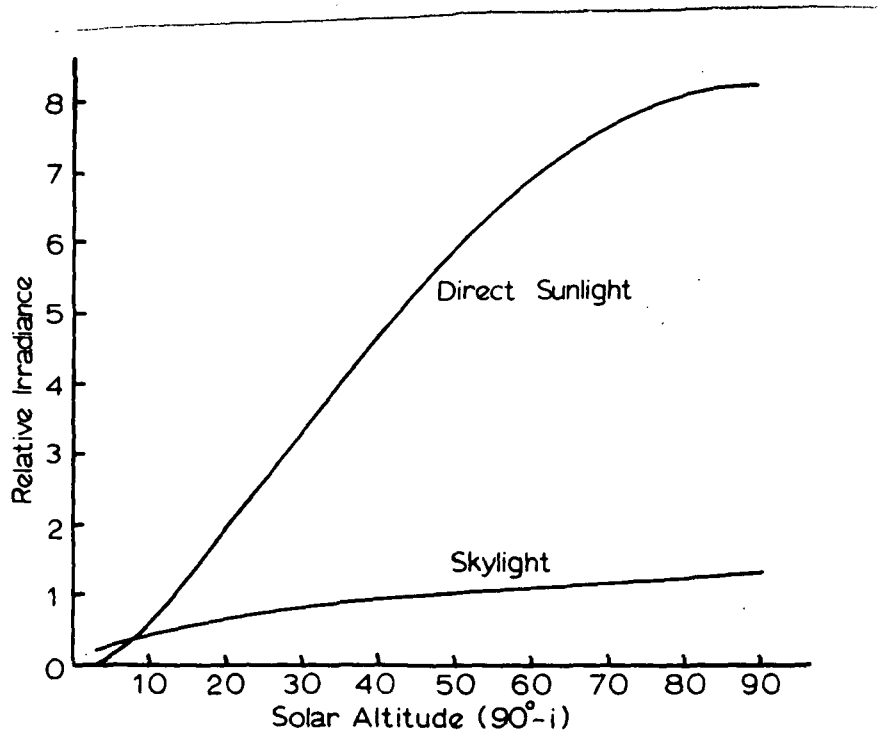

Figure 3. Direct sunlight and skylight on a horizontal plane.

ceived at the earth's surface (H) can be estimated by

$$H = H_o \exp(-KL) \qquad (1)$$

where K is the attenuation coefficient which varies with wave length, H_o is the incoming radiation at the outer atmosphere and L is the light path length (Elterman and Toolin, 1965).

Absorption of light depends on the composition of the air, mainly water vapor, carbon dioxide and ozone, and the wavelength of light. It can be seen in Figure 2, that there are several zones of selective absorption. The ultraviolet part of the sun's radiation with a wavelength of 290 nm or less is completely cut off by the atmospheric ozone layer and oxygen before it reaches the earth's surface. In the near infrared region (0.7 to 5 microns), the selective absorption is primarily due to water vapor and carbon dioxide (Holter, 1967).

The attenuation depends not only on the turbidity in the atmosphere but also on the length of path through the atmosphere. The length of the light path varies approximately as the secant of the zenith angle (i). Hence, the zenith angle (i) is involved in reducing illumination in two ways. First, the intensity on a horizontal surface is cos(i) times the intensity on a

plane normal to the radiation. Second, the path traversed by radiation through the atmosphere is greater for large angles than for the small angles. The irradiance on a horizontal plane at sea surface is

$$H_s = H_o \cos(i) \exp(-A \sec(i)) \qquad (2)$$

where A is the extinction optical thickness and includes Rayleigh attenuation, aerosol attenuation, and ozone absorption for a standard atmosphere (Elterman and Toolin, 1965).

In clean, dry, air molecular scattering is of primary importance. The scattering of very small particles of molecular dimensions is inversely proportional to the fourth power of the wavelength (Jensen, 1968) and, therefore, affects the shorter wavelengths more than the longer wavelengths. This is the reason most black and white aerial photography is taken with the minus-blue filter. As the particle sizes in the atmosphere increase, the wavelength of maximum scatter becomes less selective and extends into the green, yellow, etc., regions of the spectrum. Hence, the color of the sky changes toward cloud white as the particles increase from molecular to aerosol size. As a result, aerial photography taken under turbid atmospheric conditions requires filtering

out of more of the spectrum, including green and possibly yellow light to produce a noticable effect (Tarkington, 1966). Photographs taken in the near infrared wavelengths are better able to penetrate haze.

Light Reflection

Since the reflected light from the water surface will not contribute information on the material in the water, it should be reduced to a minimum. The incident light includes both direct sunlight and diffused skylight. The reflection of direct sunlight will be partially polarized and can be reduced from exposing the film by the proper orientation of a polarized filter. On a cloudless day, the skylight will be predominantly blue and the surface reflection of diffused light can be reduced with a minus blue filter. Figure 3 shows the effect of the sun's altitude on the irradiance of skylight and direct sunlight (Jones and Condit, 1948).

The height of the sun above the horizon is critical for water quality studies. The maximum height determines the amount of reflected light reaching the sensor while the minimum height determines light penetration into the sea. If the sea surface were calm, a single

mirror-like reflection of the sun would appear. As the sea surface is generally not smooth, the zenith angle of the sun must be greater than half the angular coverage to avoid the sun spot glare. The width of the glitter pattern about the sun's reflection is an indication of the maximum slope of the sea surface. Cox and Munk (1955) have studied roughness of the sea surface by analyzing photographs of the sun's glitter. As shown in Figure 4, a sloping water surface will require that the minimum zenith angle of the sun be at least half the angular coverage plus twice the water surface slope if the imagery is to be free of the sun's glare. The slope of waves can vary from 0° to over 90° for breaking waves. It is, therefore, necessary to select a reasonable value of slope which will eliminate most of the sun spot glare for the expected sea conditions during photography. Studies (Cox and Munk, 1954) have indicated that for a 3-knot wind the maximum slope is about 15° and about 25° for an 18-knot wind. For photographing underwater objects Faas (1960) suggests that the slope 18.5° be used. This would indicate that the sun's zenith angle at the time of imagery be at least 37° plus half the angular coverage of the sensor, if the sun's glitter is to be avoided. An alternate solution is to mount the equipment to take oblique imagery.

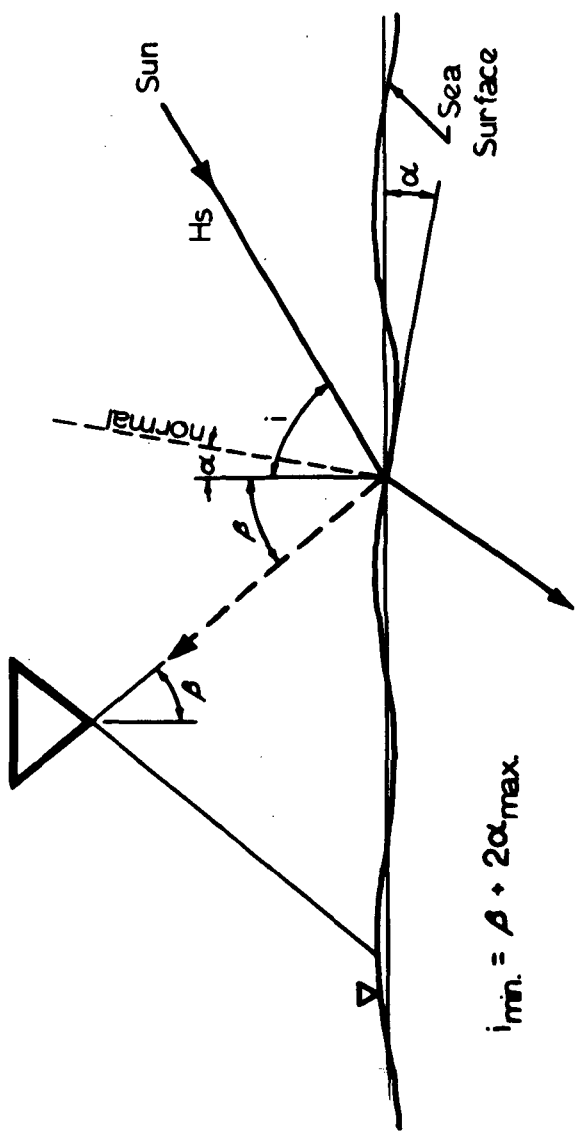

Figure 4. Sunlight reflection from a sloping water surface.

The light reaching the water surface is either reflected from or refracted through the air-sea interface. As shown in Figure 5, the incident light (H_s) is divided into that which penetrates the sea (H_w) and that which is reflected from the interface. If i is the angle of incidence of the incoming radiation and j is the angle of refraction, then sin(i)/sin(j) is equal to the index of refraction for water or about 4/3. The reflectivity of an optically flat water surface is theoretically obtained for unpolarized light from Fresnel's law (Jerlov, 1968) which gives the ratio (p_a) of reflected energy to incoming radiation and is

$$p_a = \tfrac{1}{2}\left[\frac{\tan^2(i-j)}{\tan^2(i+j)} + \frac{\sin^2(i-j)}{\sin^2(i+j)}\right] \qquad (3)$$

where the terms inside the brackets are for the components of light parallels and perpendicular to the plane of incidence from 0 to 90 degrees is shown in Figure 5. It can be seen that the reflectivity increases rapidly when the angle of incidence exceeds 60 degrees. The irradiance (H_w) below the sea surface and normal to the beam is

$$H_w = (1 - p_a)H_s\sec(j) \qquad (4)$$

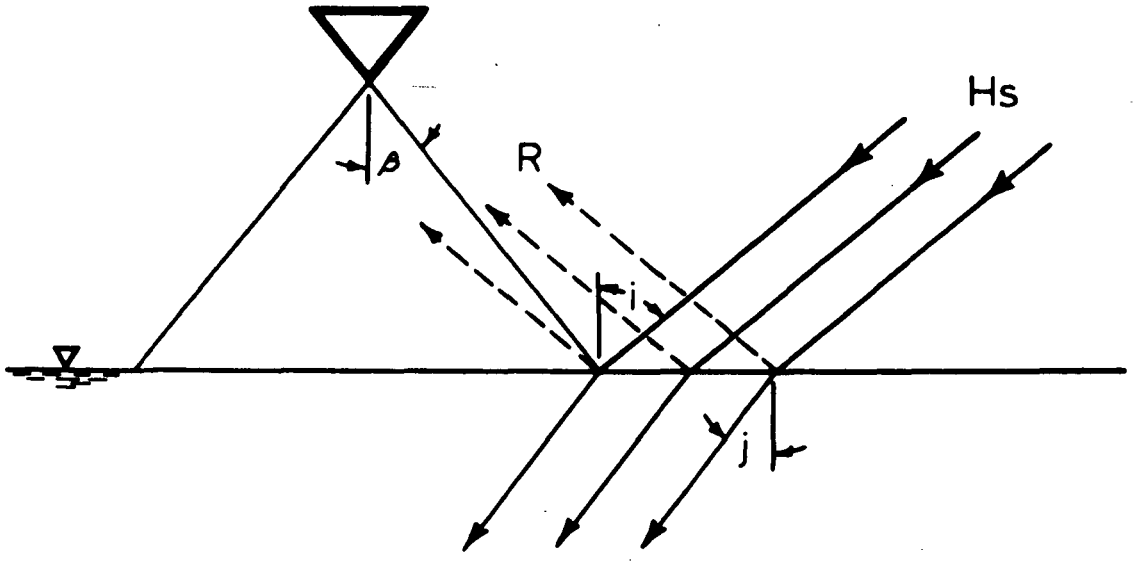

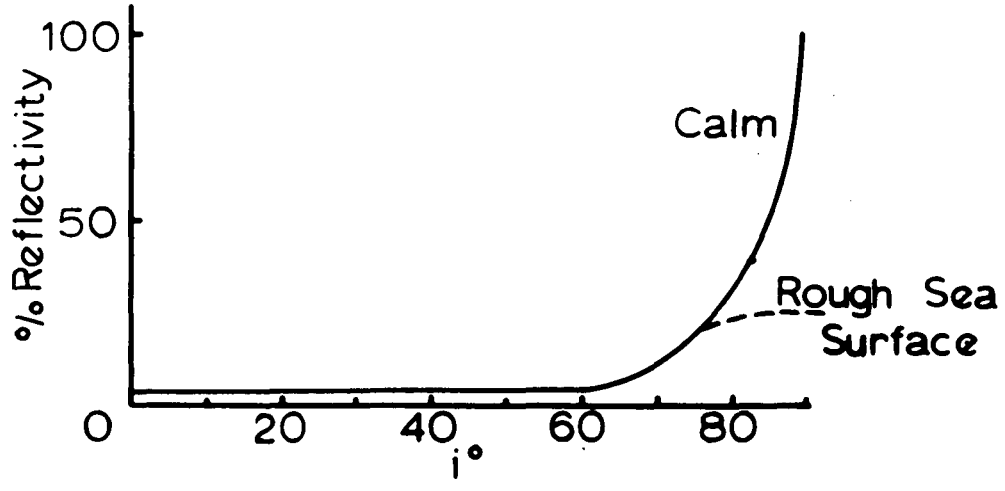

Figure 5. Light penetration into the sea.

Light Attenuation in the Sea

The radiation that penetrates the surface of the sea is progressively diminished by extinction as it travels through the water. The attenuation of light is caused by scattering and absorption. By applying Lambert's and Beer's laws for monochromatic light the intensity H_z at some depth z below the sea surface is given by

$$H_z = H_w \exp(-C\ z\ \sec(j)) \tag{5}$$

$$C = a + bW \tag{6}$$

where C is the attenuation coefficient for sea water and contaminant, 'a' is the sea water attenuation coefficient, b is the contaminant absorption coefficient and W is the contaminant concentration. The attenuation coefficients for sea water and Kraft pulp waste are shown in Figure 6. Minimum attenuation of sea water occurs at about 540 nm while the minimum for the waste is about 700 nm.

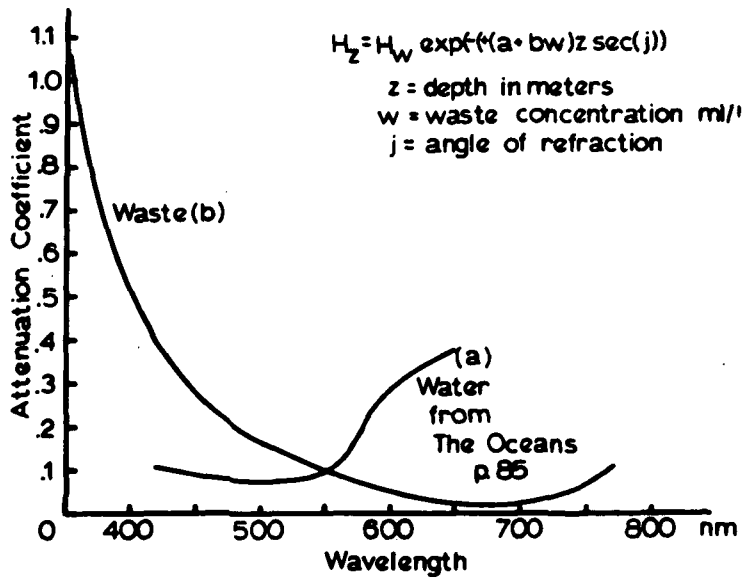

Figure 6. Typical attenuation coefficients.

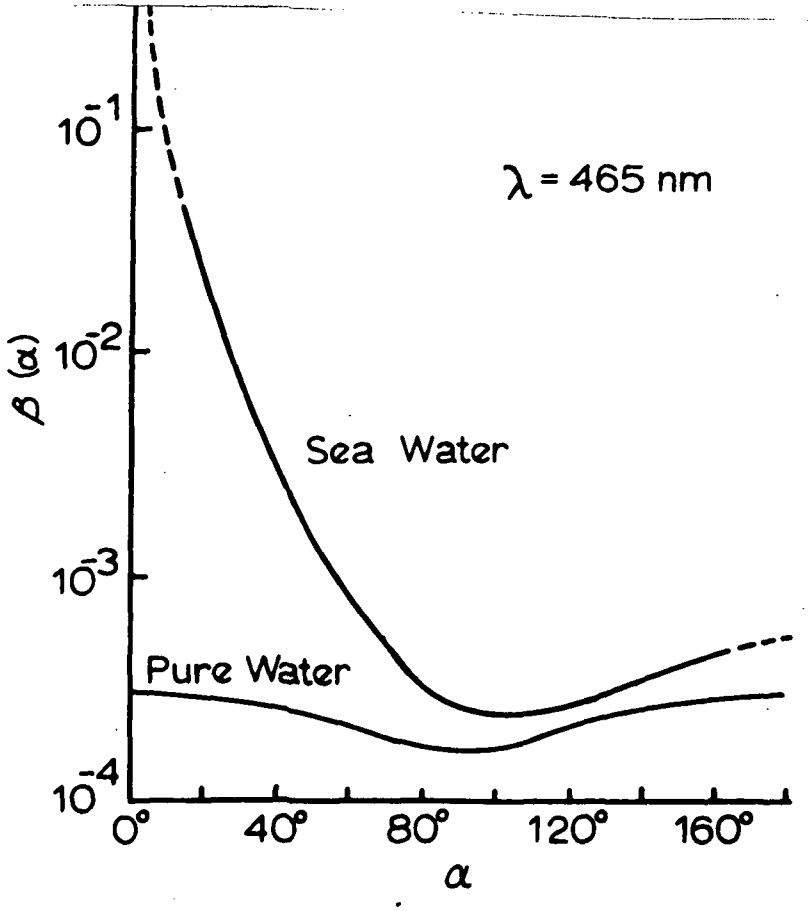

Figure 7. Volume scattering function.

Light Scattering in the Sea

The attenuation coefficients of both sea water and the contaminant can be divided into attenuation due to absorption and attenuation due to scattering. The scattering of light in a turbid medium is caused by reflection and diffraction of light rays by small particles of suspended matter and colloidal solutions. As in the atmosphere, if the size of the particles is small compared to the wavelength of light, then the intensity of the scattering light is inversely proportional to the wavelength to the n^{th} power. The exponent n decreases with increasing particle size from the value of four for pure water to approaching zero for coarse suspended matter (Jensen, 1968). Thus for solutions with small particles, the blue light has the maximum scatter, while for solutions with larger particles all colors are scattered about the same amount.

By definition of the volume scattering function $\beta(\alpha)$, the scattered light intensity (dJ) from an incremental volume dV is

$$dJ = H_z \beta(\alpha)\, dV \qquad (7)$$

where α is the angle between the incident beam and the scattered light.

Figure 7 shows the variation in the volume scattering function for both sea water and pure water (Jerlov, 1964). It can be seen that the curve for pure water is symmetrical with a minimum at α equal to 90 degrees. The scattering function for sea water varies greatly with α.

The variation of the scattering angle (α) on an aerial photograph is shown in Figure 8. The angle between the incoming direct light in the sea and the scattered light reaching the sensor changes with position; hence, the intensity of scattered light from below the sea surface will also vary. For a vertical photograph taken with a 6-inch aerial camera when the sun's zenith is 55 degrees, the angle α would vary from about 110 degrees to 170 degrees.

Figure 9 is a plot of data taken from work by Tyler and Richardson (1958). In this study a nephelometer was used to measure the radiant intensity scattered from a volume for various scattering angles (α). A contaminant of skim milk was added at various concentrations. The light scattering for the various solutions is directly related to concentration of the contaminant.

For scattering by large particles, the intensity of the scattered light is proportional to the particle sur-

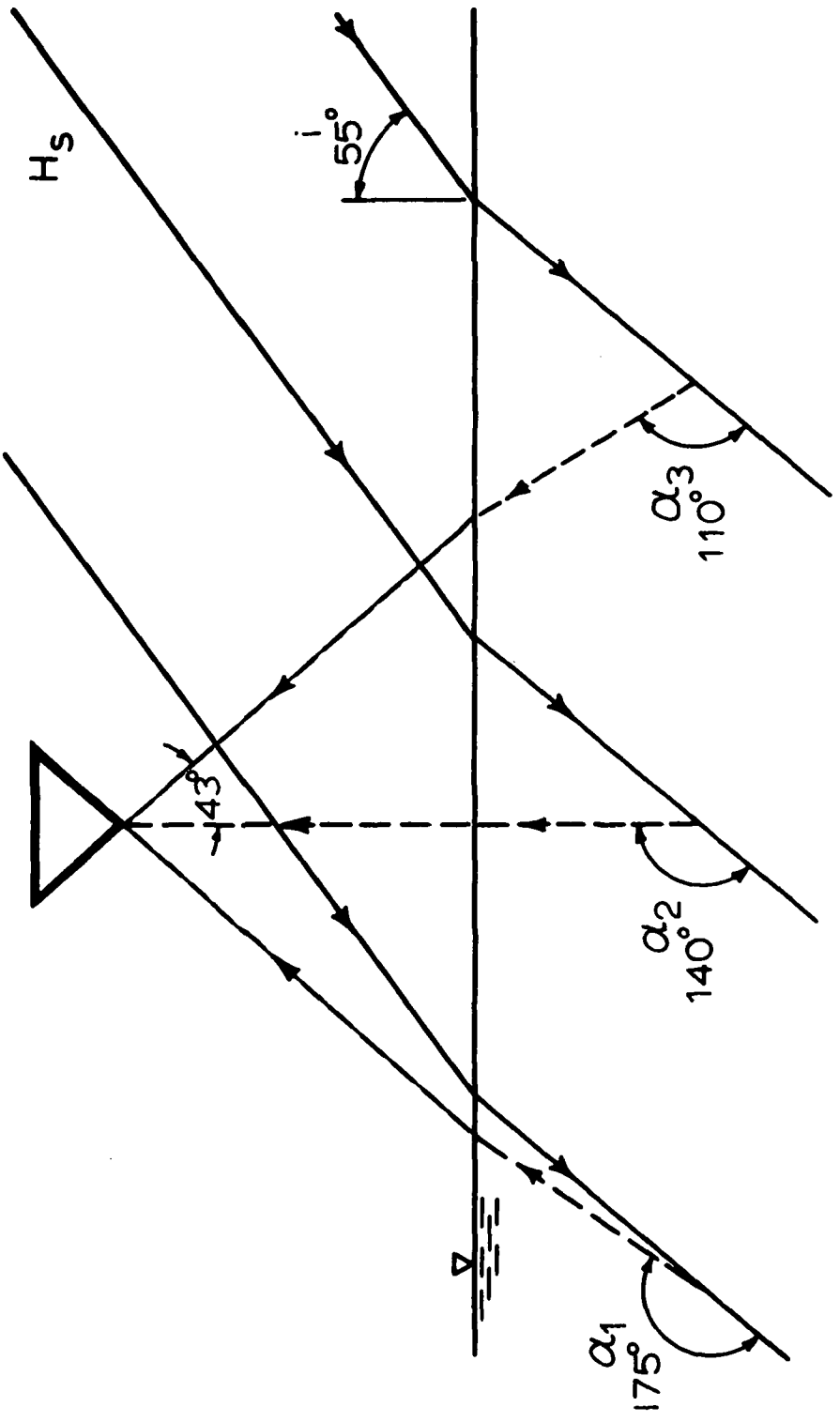

Figure 8. Variation in the scattering angle.

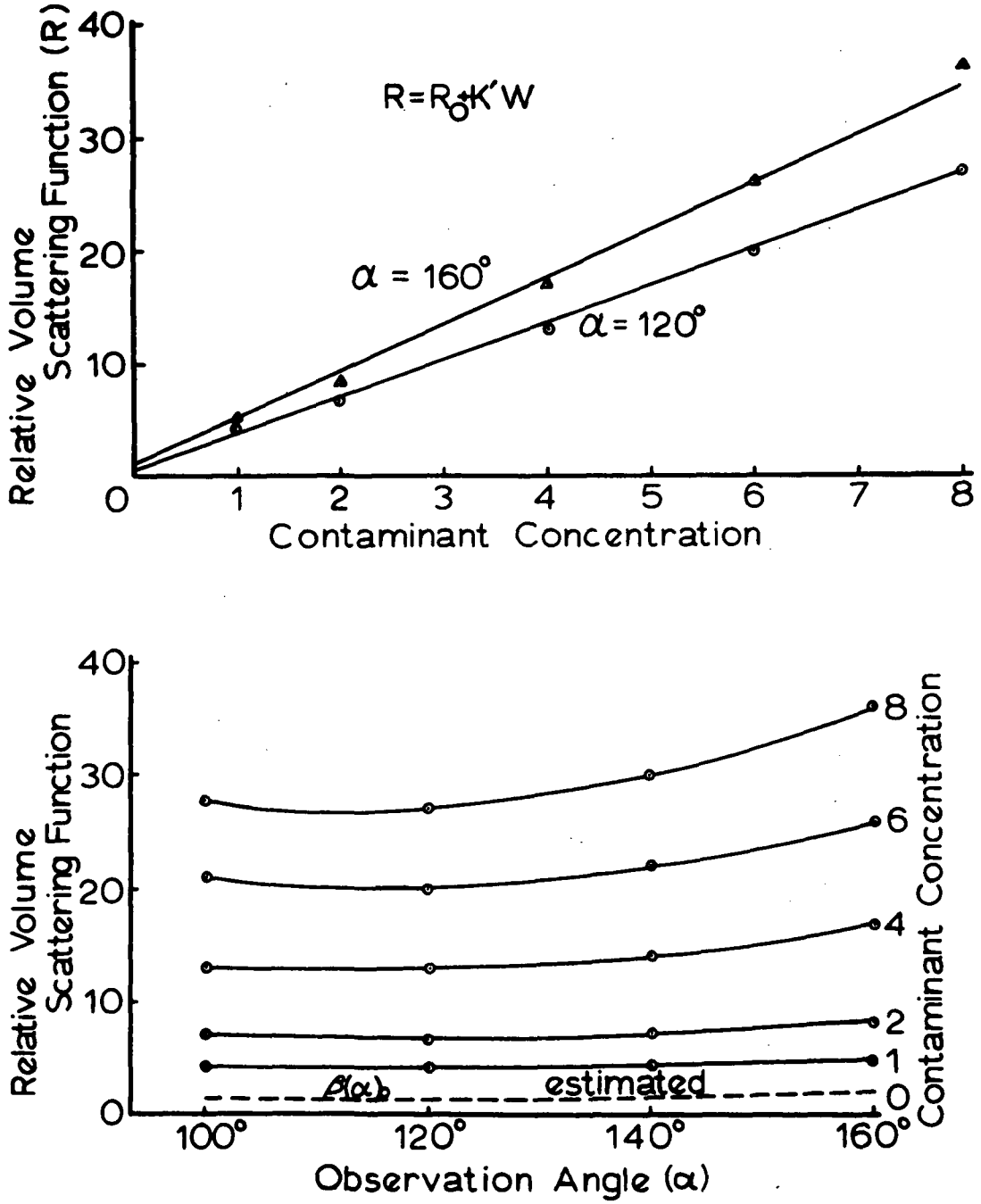

Figure 9. Effect of contaminant on the scattering function.

face area that is exposed to the incident beam (Jerlov, 1968). If the particle size is uniform, then the intensity of the scattered light is proportional to the waste concentration. In the upper plot in Figure 9 the volume scattering function is shown as a linear function of the waste concentration. From the lower plot in Figure 9, it can be seen that the function $\beta(\alpha)$ can be approximated by

$$\beta(\alpha) = \beta_o(\alpha)(1 + K'W) \tag{8}$$

where $\beta_o(\alpha)$ is the volume scattering function of the sea water, K' is a constant for a particular waste and W is the waste concentration.

As shown in Figure 10, if R is the distance from the volume element (dV) to the point where the scattered light strikes the surface and $d\Omega$ is the solid angle formed at the surface by dV, then

$$dV = R^2 d\Omega dR \tag{9}$$

In addition, the emerging ray of scattered light from the incremental volume will be augmented by diffused light of almost uniform intensity in all directions. As the intensity of the light which is scattered for the second time, will be approximately three orders of magnitude less than that of the direct lighting, the addi-

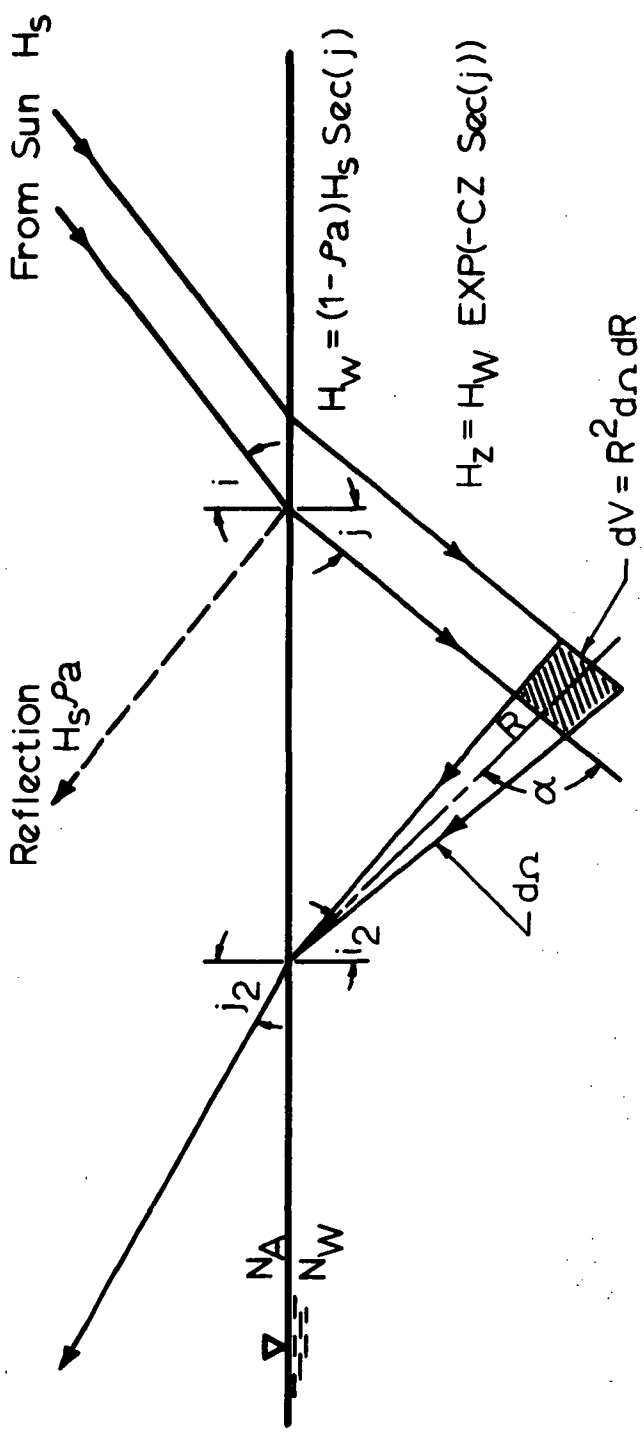

Figure 10. Light from the sea.

tion of the rescattered light to the emerging ray will not be considered. The intensity of the emerging ray dJ will be reduced by the absorption and scattering of the water and particles. From the inverse square law, the irradiance from the scattering volume incident on a normal plane to the beam at the surface is

$$dH_a = \frac{dJ}{R^2}\exp(-CR) \tag{10}$$

By combining equations and integrating, the irradiance at the surface is

$$H_a = \frac{H_o\beta_o(\alpha)\cos(i)(1 - pa)\exp(-A\ \sec(i))d\Omega}{\cos(i_2)\cos(j)}$$

$$\int (1 + K'W)\exp(-(a + bW)(\sec(j) + \sec(i_2))z)dz \tag{11}$$

If the waste concentration is a known function of the depth (z), then Equation 11 can be integrated numerically. However, if the waste field forms a relatively stable layer at the surface and the waste concentration is approximately uniform throughout the depth of this layer, then Equation 11 can be integrated directly.

If the waste concentration is not a function of depth and $\exp(-(a + bW)z(\sec(j) + \sec(i_2))$ approaches zero, Equation 11 reduces to

$$H_a = \frac{(1 + K'W)H_o\beta_o(\alpha)\cos(i)(1 - pa)\exp(-A \sec(i))d\Omega}{(a + bW)\cos(i_2)\cos(j)(\sec(i_2) + \sec(j))} \quad (12)$$

Evaluation of $\exp(-Cz(\sec(j) + \sec(i_2)))$ is shown in Figure 9 for the green, red, and infrared regions of the spectrum. The expression was evaluated for values of the angles j and i_2 other than those listed in Figure 11, however, the expression was relatively insensitive to changes in these angles. Average values of attenuation coefficients were selected from Figure 6. It can be seen from the upper plot in Figure 11 that 90% of the light returned in the infrared region is from the upper half meter of water. In the red and green bands the depth above which 90% of the light is returned is a function of the waste concentration. From the lower plot in Figure 11, it can be seen that in the open sea 50% of the light in the red and green bands is returned from the upper two and four meters, respectively.

Radiance from the Sea

From Equation 12 the radiance (N_W) from the scattering volume below the sea surface is

$$N_W = \frac{H_a}{d\Omega} \quad (13)$$

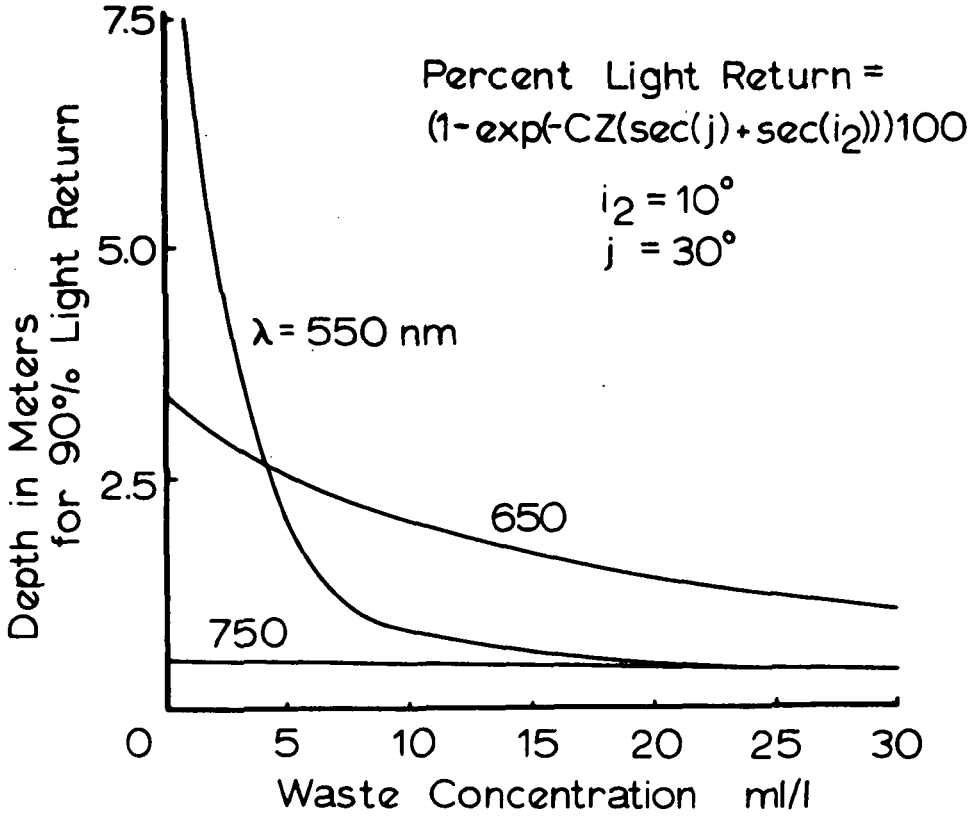

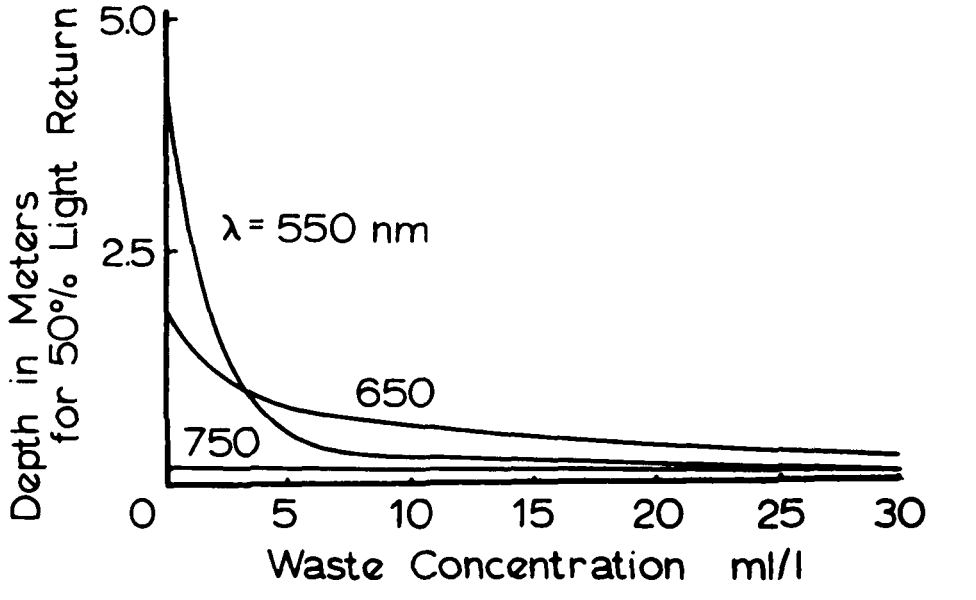

Figure 11. Depth of light return from the sea.

The light spreads into a larger solid angle when passing through the sea-air interface (Jerlov, 1968) and the radiance in air is

$$N_a = \frac{N_w}{n^2}(1 - p_w) \tag{14}$$

where n is the refractive index of water and p_w is the reflectivity of light at the interface.

In addition to the upward radiance from the sea, the light reaching the photographic sensor includes skylight reflection, direct sunlight reflection and path radiance intensity. Reflectance of skylight from a rough sea surface can be approximated by a Lambert reflector while the direct sunlight is reflected specularly. Skylight radiance reflected from the surface is given by

$$N_{sky} = p_s \frac{Hsky}{\pi} \tag{15}$$

where p_s is reflectivity of the skylight and was found by Burt (1953) to be approximately 0.066. The skylight irradiance (Hsky) is a function of solar altitude, atmospheric scattering and wavelength of light. Path radiance intensity is a function of the length of sight ray, angle between sight and sun rays, atmospheric conditions and wavelength. For a clear atmosphere, skylight irradiance

will be due predominently to Rayleigh scattering and will have greatest influence on the shorter wavelengths. The reflection of direct sunlight is mathematically easier to estimate in magnitude by Fresnel's equations but its direction is difficult to predict without knowing the surface configuration of the sea. Since the Fresnel's equations are nearly independent of wavelength, the magnitude of direct sunlight reflection will be proportional to each other in spectral bands of the sensor.

If N is the radiance from the sea surface and the path radiance is neglected, then the radiance at the sensor is

$$N_c = N \exp(-E \sec(j_2)) \tag{16}$$

where E is the extinction optical thickness for the attenuation by the atmosphere from the sea to the camera. E is, therefore, a function of flying height and wavelength. N includes the skylight reflection (N_{sky}), direct sunlight reflection (N_d), and upward radiance from the sea and the waste (N_a) or

$$N = Nsky + N_d + N_a \tag{17}$$

By combining Equations 12, 13, 14, 15, and 17 the radiance N is equal to

$$N = p_s \frac{Hsky}{\pi} + N_d +$$

$$\frac{(1 - p_w)(1 + K'W)\beta_o(\alpha)H_o\exp(-A \sec(i))\cos(i)(1 - pa)}{n^2(a + bW)\cos(j)\cos(i_2)(\sec(i_2) + \sec(j))} \tag{18}$$

The first term on the right is the skylight reflection, the second term is direct sunlight reflection and the last term is the uplighting from the sea (Na).

Equation 18 can be expanded by writing the equation for each of the spectral bands. The subscripts g and r refer to the bands of maximum absorption and scatter, respectively.

$$N_g = K_4 p_s \frac{Hsky}{\pi} + K_5 N_d + K_6 Y(\exp(-A_g \sec(i))) \frac{(1 + K'_g W)}{a_g + b_g W} \beta_o(\alpha) \tag{19}$$

$$N_r = K_7 p_s \frac{Hsky}{\pi} + K_8 N_d + K_9 Y(\exp(-A_r \sec(i))) \frac{(1 + K'_r W)}{a_r + b_r W} \beta_o(\alpha) \tag{20}$$

A typical spectral signature of both the open sea and the waste field is shown in Figure 12. The effect of skylight, direct sunlight, and waste on the spectral signature is shown in the figure. Whenever possible, direct sunlight reflection from the water surface should

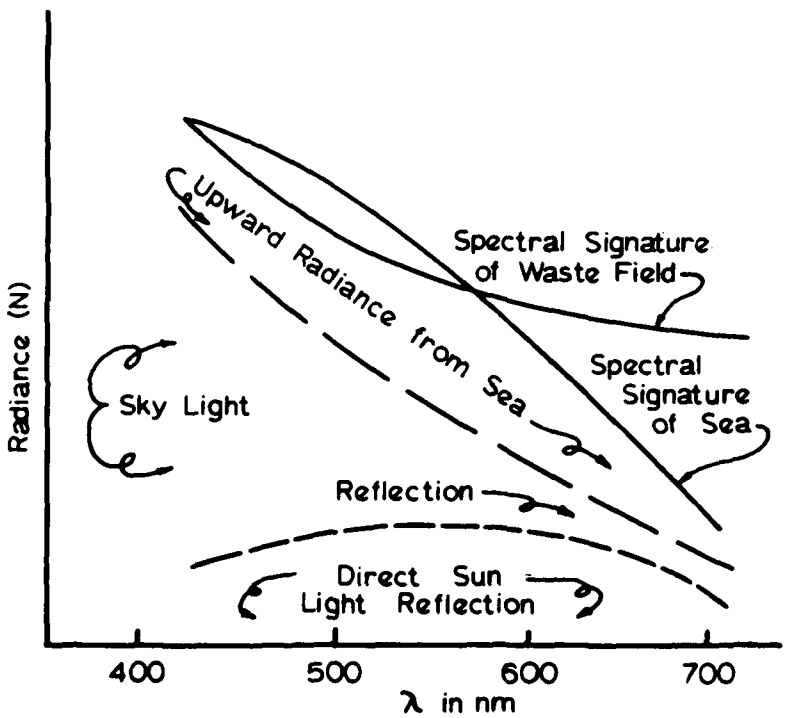

Figure 12. Typical spectral signature.

be avoided as it will cause interference with the data processing. Hence, the second term on the right of the three equations is zero. As skylight is predominantly blue

$$K_4 \sim 0, \quad K_7 \sim 0$$

Rewriting Equations 19 and 20

$$N_g = K_6 Y \frac{(1 + K_g'W)}{a_g + b_g W} \exp(-A_g \sec(i)) \tag{21}$$

$$N_r = K_9 Y \frac{(1 + K_r'W)}{a_r + b_r W} \exp(-A_r \sec(i)) \tag{22}$$

Where Y is a constant for the two bands at a point and is equal to

$$Y = \frac{H_o(1 - pw)(1 - pa)\cos(i)\beta_o(\alpha)}{n^2 \cos(j)\cos(i_2)(\sec(i_2) + \sec(j))} \tag{23}$$

The Y term can be eliminated by taking the ratio (Rp) of the radiance in the two bands

$$Rp = K_{10} \frac{1 + K_r'W}{1 + K_g'W} \frac{a_g + b_g W}{a_r + b_r W} \exp(-(A_r - A_g)\sec(i)) \tag{24}$$

where K_{10} is a constant.

$\frac{1 + K'_r W}{1 + K'_g W}$ is the scattering coefficient ratio

and shows the effect of scattering on the composition of the scattered light. As the particle size is relatively large compared to the wavelength of light, the scattered light is of nearly the same composition as the incident light. Therefore, this term is approximately equal to one.

The term $\frac{a_g + b_g W}{a_r + b_r W}$ represents the change in light composition due to the selective absorption of the contaminant and the sea water.

$\exp(-(A_r - A_g)\sec(i))$ is the atmospheric attenuation ratio and shows the effect of the sun's altitude on the incident light composition.

From Equation 24, the ratio at the sea surface (Rph) is

$$Rph = Rp \exp((A_r - A_g)\sec(i)) = K_{10}\frac{a_g + b_g W}{a_r + b_r W} \qquad (25)$$

Photographic Measurement of Light

The aerial photograph is a light detector and can be used to measure the light return from objects. As shown in Figure 13, j_2 is the angle between the ray to the camera and the vertical. If the angle between the ray and the camera axis is represented by c, then by geometry

$$dA = dA' \left[\frac{Z_o}{f}\right]^2 \left[\frac{\cos(c)}{\cos(j_2)}\right]^3 \tag{26}$$

where dA is the area on the sea surface included in the densitometer aperture area dA' on the photographic film, Z_o is the flying height and f is the focal length of the camera. The solid angle subtended by the lens of diameter D is

$$d\Omega = \frac{\pi}{4} \left[\frac{D\cos(j_2)}{Z_o}\right]^2 \cos(c) \tag{27}$$

The radiant flux (dp') collected by the camera lens is

$$dp' = N_c dA \cos(j_2) d\Omega \tag{28}$$

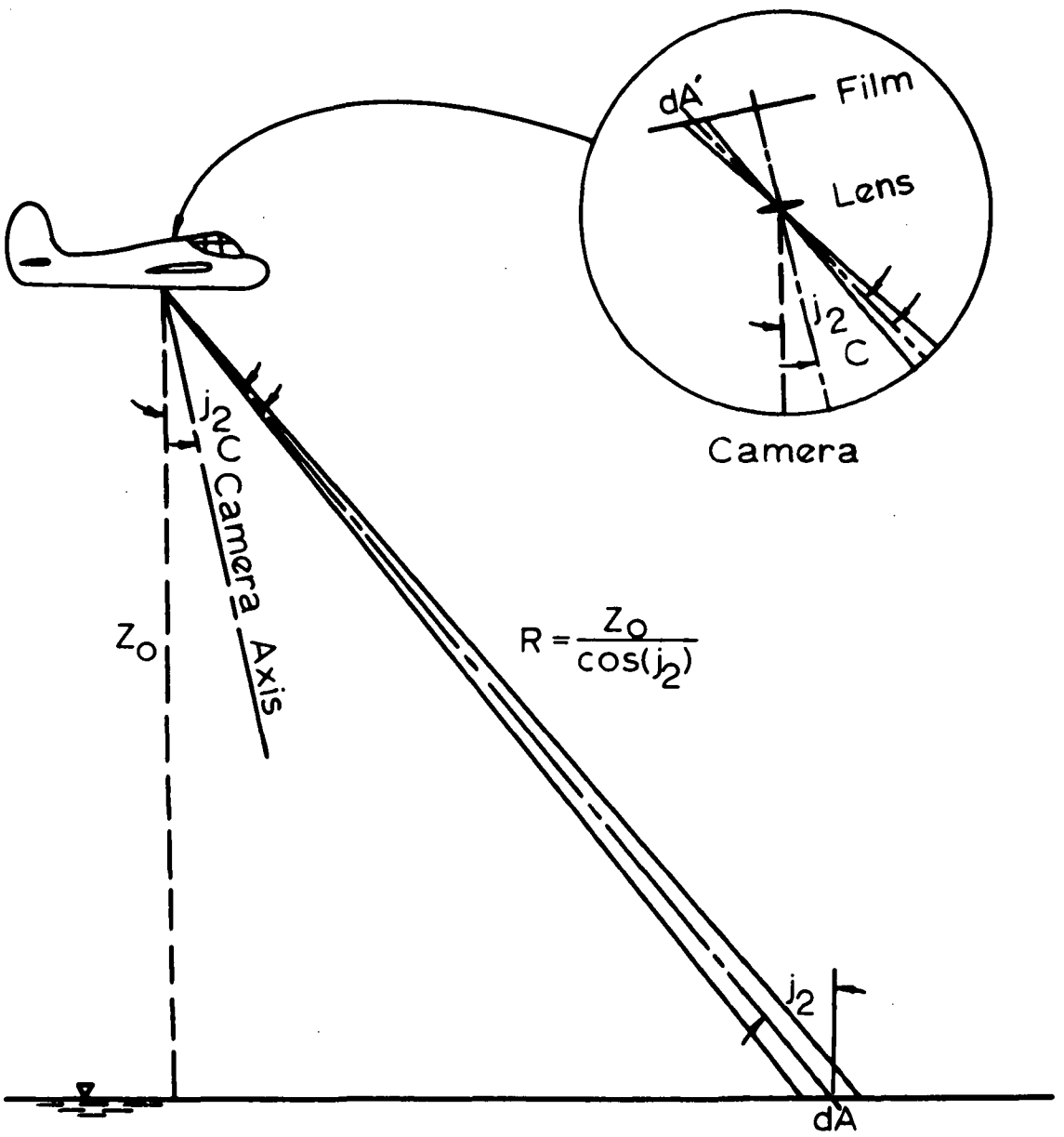

Figure 13. Geometry of exposure calculation.

The irradiance of the film image is

$$H' = \frac{dp'}{dA'} = K_{12}\frac{TR\ N_c \cos^4(c)}{(FNO)^2} \qquad (29)$$

where K_{12} is a constant, FNO is the relative aperture of the lens (f/D), TR is the lens transmittance and N_c is the object radiance at the camera.

The photographic exposure (EX) is the product of image irradiance (H') or the rate at which energy is incident upon a unit area of the film and the time (TIM) during which it acts. The equation

$$EX = H' \times TIM \qquad (30)$$

indicates that there are many combinations of H' and TIM that will give the same exposure. This is known as the Reciprocity Law and is correct for normal aerial photography where extremes in exposure times are not employed.

The density of a film is defined as the common logarithm of the reciprocal of the transmittance or the logarithm of the ratio of incident light on the film and the transmitted light through the film. The relationship between film density and exposure is shown by the characteristic curves of a film. The curve is a plot of log exposure against film density for a particular development.

A typical characteristic curve is shown is Figure 14 (American ..., 1968).

The characteristic curve can be divided in three parts; the lower part of the curve AB which is concaved upward is known as the toe, the straight line portion of the curve BC, and the top part of the curve CD which is concaved downward and is known as the shoulder region. The toe of the characteristic curve approaches a horizontal line at some value of density greater than zero. This value represents the density of the base of the film.

The slope of the straight line portion of the characteristic curve is known as the film gamma. The greater the gamma the greater the contrast or the greater the difference in densities on a given photograph. The gamma is a characteristic of the film but varies within limits with different development time. The speed or exposure index of the film is indicated by the horizontal position of the characteristic curve along the exposure axis.

If the exposure of the film is on the straight line portion of the D log E curve, then the film density can be expressed by

$$D(x, y) = M + G \ln(EX) \tag{31}$$

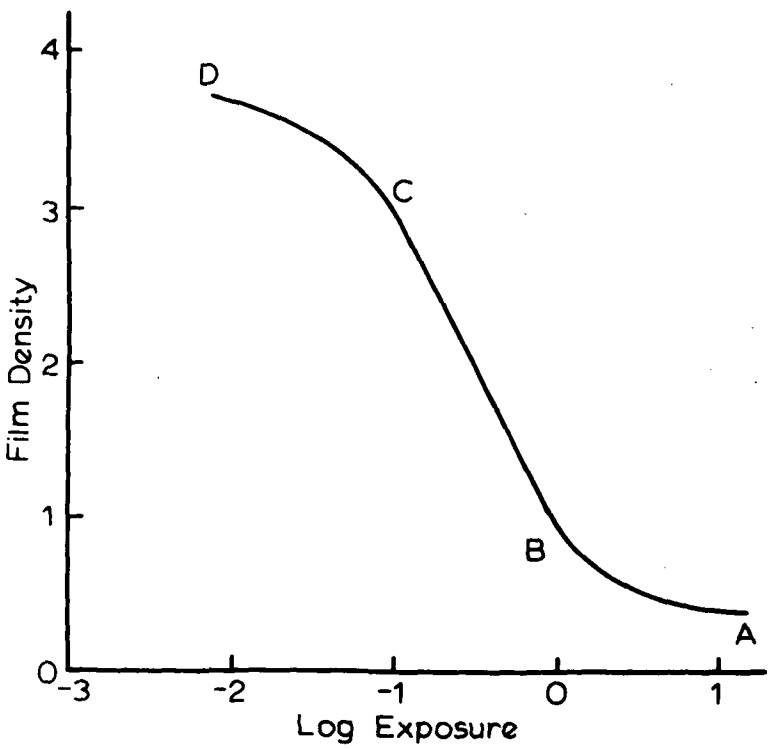

Figure 14. Typical characteristic curve of an aerial positive film.

D(x, y) is the film density at the point on the photo with film coordinates x and y, M is a constant representing the film speed, G is the gamma or contrast of the film and EX is the exposure. If the two regions of the spectrum are measured with two cameras, the camera settings can be adjusted for optimum exposure in each band. By using high contrast developer and/or film, the sensitivity of the film density to the contaminant concentration can be increased.

Combining Equations 30 and 31 and solving for the image irradiance

$$H' = \frac{K_{13}}{TIM} \exp((D(x, y) - M)/G) \tag{32}$$

The radiance from the sea as measured at the camera station is determined from Equations 29 and 32

$$N_c = \frac{K_{14}(FNO)^2 \exp((D(x, y) - M)/G)}{(TIM)(TR)\cos^4(c)} \tag{33}$$

By including the atmospheric attenuation, but neglecting light path radiance in the atmosphere, the radiance at the sea surface (N) is equal to

$$N = \frac{K_{15}(FNO)^2}{(TIM)(TR)\cos^4(c)} \exp(D(x, y)/G + E \sec(j_2)) \tag{34}$$

where the term exp(-M/G) has been included in the constant (K_{15}). The factor exp(E sec(j_2)) compensates for the atmospheric attenuation of the light from the sea surface to the camera. Writing Equation 34 for two spectral bands:

$$N_g = \frac{K_{17}(FNO)^2 \exp(D_g(x, y)/G_g + E_g \sec(j_2))}{(TIM)(TR_g)\cos^4(c)} \qquad (35)$$

$$N_r = \frac{K_{18}(FNO)^2 \exp(D_r(x, y)/G_r + E_r \sec(j_2))}{(TIM)(TR_r)\cos^4(c)} \qquad (36)$$

The ratio (R) of the radiance in the two bands is obtained by dividing Equation 36 and 35

$$R_p = \frac{N_r}{N_g} = K_{19}\exp((D_r(x, y)/G_r - D_g(x, y))/G_g + (E_r - E_g)\sec(j_2)) \qquad (37)$$

As in Equation 25, the value of R_{ph} is defined as

$$R_{ph} = R_p \exp(A_r - A_g)\sec(i)$$

$$= K_{19}\exp((D_r(x, y)/G_r - D_g(x, y))/G_g + (E_r - E_g)\sec(j_2)$$

$$+ (A_r - A_g)\sec(i)) \qquad (38)$$

where angle i is the angle of incidence for the direct sunlight and A_r and A_g are the extinction optical thickness of a standard atmosphere for the maximum absorption and scatter bands of the water respectively.

If Rpho is the ratio of the radiance from the sea for the two bands where no contaminant is present and this value is adjusted for the atmospheric attenuation as in Equation 38. R_{pho} can be estimated by the following regression model for any point.

$$R_{pho} = B_o + B_1 SUNR + \varepsilon \tag{39}$$

In this equation B_o and B_1 are regression coefficients to be determined by a least squares fit of the model to the data points outside the contaminant area. Imagery for model 39 should be taken at the same altitude and nearly the same time as the imagery that is being processed. SUNR is the angle between the ray from the sea to the camera station and the direct sunlight ray reflected from a horizontal surface.

The ratio anomaly (RA) is defined as

$$RA = R_{ph} - R_{pho} \tag{40}$$

and is the variation in the ratio of two bands of light returned from within the sea due to the presence of contaminant. The value of the ratio anomaly is determined from Equations 38 and 39.

Contaminant Concentrations

The relationship between the value RA and the concentration W can be developed from Equation 25 as

$$RA = K_{10}\left[\frac{(a_r b_g - a_g b_r)W}{a_r(a_r + b_r W)}\right] \qquad (41)$$

Evaluation of the term in the brackets of Equation 41 is shown in Figure 15. The relationship between value of RA and the contaminant concentration is a function of the sea water attenuation coefficients and the waste absorption coefficients. Average values of these coefficients were selected from Figure 9. The upper curve in Figure 18 is for the ratio of red to green radiance. For comparison two other curves were included. The lower curve is for the ratio of infrared to red and the center curve is for the ratio of infrared to green. While the ratio of red to green radiance is the most sensitive to changes in waste concentration, it is also the ratio with the greatest

$$f(a,b) = \frac{(a_r b_g - a_g b_r)W}{a_r^2 + a_r b_r W}$$

Curve No.	Band Subscripts		Evaluated For
	r	g	green at 550nm
1	red	green	red at 650nm
2	infrared	green	infrared at 750nm
3	infrared	red	

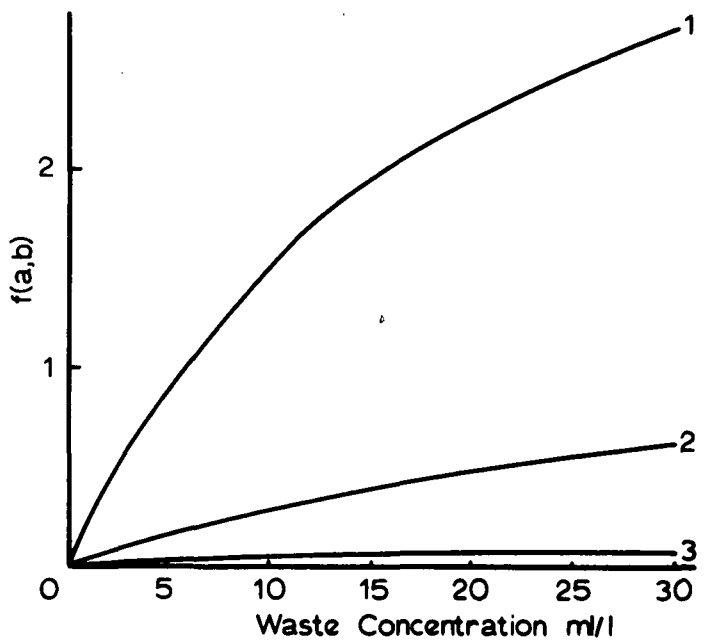

Figure 15. Spectral response curves.

interference to skylight reflection and light path radiance. Curves such as those shown in Figure 15 are useful in predicting the response of different bands for measuring contaminant concentrations; however, interference must be considered.

From Equation 41 the contaminant concentrations can be expressed as

$$W = C_1(RA) + C_2(RA)^2 + \ldots \qquad (42)$$

where C_1 and C_2 are coefficients. Thus, Equation 42 provides a relationship between the value RA which is measured by the remote sensor and the water quality parameter, W, which in this case represents a contaminant concentration.

CONCLUSION

Remote Sensing can be a valuable tool for a waste management program. By monitoring both the polution sources and the environmental quality the interactions between the components of the esturaine system can be better understood. Remote sensing can provide comprehensive, quantitative water quality data of a large area which is usually impossible to acquire by conventional method in this dynamic environment. As new calibrated, multichannel

sensors are being developed, the need for in situ sampling will be reduced.

Variations in light returned from the water column can under certain conditions be quantitatively related to water quality parameters. Thus, remote sensing can be used to 1) detect pollution sources, 2) map the zone of influence of the waste source an the water quality and 3) estimate the magnitude of the water quality parameters. Remote sensing techniques can also be utilized to determine waste disposal design parameters such as diffusion coefficients and circulation patterns. Many of the subtile changes in vegetative patterns and density caused by extended exposure to low waste concentrations might be detected by a continuous monitoring program.

By understanding the response of the environment to various waste loadings, the effect of additional pollution can be predicted and degradation of the water quality prevented by proper waste management decisions.

REFERENCES

Allen Hancock Foundation. 1964. An investigation on the fate of organic and inorganic wastes discharged into the marine environment and their effects on biological productivity. Los Angeles, University of Southern California. 118 p. (California State Water Quality Control Board Publication 29).

American Society of Photogrammetry. 1968. Manual of color aerial photography. Menasha, George Banta Company. 550 p.

American Society of Photogrammetry. 1960. Manual of photographic interpretation. Menasha, George Banta Company. 868 p.

Burgess, F. J. and W. P. James. 1970. An aerial photographic tracing of pulp mill effluent in marine waters. Federal Water Quality Office, EPA, Water Pollution Control Research Series 12040EBY, Grant WP-00524. 152 p.

Burgess, F. J. and W. P. James. 1971. Airphoto analysis of ocean outfall dispersion. Federal Water Quality Office, EPA, Water Pollution Control Research Series 16070ENS. 290 p.

Burt, Wayne V. 1953. A note on the reflection of diffusion radiation by the sea surface. Transactions, American Geophysical Union 34 (2): 199-200.

Cox, C. and W. Munk. 1954. Measurement of the roughness of the sea surface from photographs of the sun's glitter. Journal of the Optical Society of America 44: 838-850.

Cox, Charles and Walter Munk. 1955. Some problems in optical oceanography. Journal of Marine Research 14 (1): 63-78.

Elterman, Louis and Robert B. Toolin. 1965. Atmospheric optics. In: Handbook of Geophysics and Space Environment, ed. by Shea L. Valley, Cambridge, Air Force Cambridge Research Laboratories. p. 7.1-7.36.

Faas, V. A. 1960. The procurement of aerial photography of underwater objects. In: Manual of photographic Interpretation, American Society of Photogrammetry, Menasha, George Banta Company. p. 96.

Fisher, Davis, and Sousa. 1966. Fresh-water springs of Hawaii from infrared images. U. S. Geological Survey Hydrologic Investigations Atlas HA-218. Washington, D. C.

Fritz, N. L. 1967. Optimum methods for using infrared-sensitive color films. Photogrammetric Engineering 33: 1128-1138.

Holter, Marvin R. 1967. Infrared and multispectral sensing. BioScience June. p. 376-383.

Hutchinson, G. E. 1957. A treatise on limnology. Vol. 1. New York, John Wiley and Sons, Inc. 1015 p.

Ichiye, T. and N. B. Plutchak. 1966. Photodensitometric measurements of dye concentration in the ocean. Limnology and Oceanography 2: 364-370.

James, W. P. and F. J. Burgess. 1969. The use of photogrammetry in predicting outfall diffusion. National Council for Air and Stream Improvement Technical Bulletin No. 231. p. 2-26.

James, W. P. and F. J. Burgess. 1970. Ocean outfall dispersion. Photogrammetric Engineering Journal 36 (12): 1241-1250.

James, W. P. and F. J. Burgess. 1971. Pulp mill outfall analysis by remote sensing techniques. Journal of the Technical Association of the Pulp and Paper Industry. 54 (3): 414-418.

Jensen, Niels. 1968. Optical and photographic reconnaissance systems. New York, John Wiley and Sons, Inc., 211 p.

Jerlov, N. G. 1964. Optical classification of ocean water. In: Symposium on Physical Aspects of Light in the Sea, ed. J. E. Typer, Honolula, University of Hawaii Press. p. 45-49.

Jerlov, N. G. 1968. Optical oceanography. Amsterdam, Elseview Publishing Company. 194 p.

Jones, L. A. and H. R. Condit. 1948. Sunlight and skylight as determinants of photographic exposure. Optical Society of America 38: 123-178.

Keller, Morton. 1963. Tidal current surveys by photogrammetric methods. U. S. Coast and Geodetic Survey, Technical Bulletin 22. 20 p.

Keller, M. and G. C. Tewinkel. 1966. Space resection in photogrammetry. U. S. Coast and Geodetic Survey Technical Bulletin 32. 10 p.

Neumaier, G., F. Silvestro, H. Thung, and R. Frank. 1967. Project aqua-map development of aerial photography as an aid to water quality management. Buffalo, Cornell Aeronautical Laboratory, Inc. (Contract No. HC-9768 of the State of New York Conservation Department).

Ory, T. R. 1965. Line scanning reconnaissance systems in land utilization and terrain studies. In: Third symposium on remote sensing of environment. Ann Arbor, University of Michigan. p. 393-398.

Piech, K. R. and J. E. Walker. 1971. Aerial color analyses of water quality. National Water Resource Engineering Meeting, Phoenix, January, ASCE meeting repring 1327.

Romanovsky, V. 1966. Coastal currents. In: Proceedings of the Third International Conference on Advances in Water Pollution Research, Munich. Baltimore, Port City Press, Inc. Vol. 3, p. 290-292.

Scherz, James P. 1967. Aerial photographic techniques in pollution detection. Doctoral dissertation. Madison, University of Wisconsin. 82 numb. leaves. (Microfilm)

Silvestro, F. B. and K. R. Piech. 1969. Development of Aerial photography as an aid to water quality management. Cornell Aeronautical Laboratory. Final Report VT-2614-0-1.

Strandberg, C. H. 1966. Water quality analysis. Photogrammetric Engineering 32 (2): 234-248.

Strandberg, C. H. 1967. Aerial discovery manual. New York, John Wiley and Sons. 249 p.

Sverdrup, H. V., M. W. Johnson and R. H. Fleming. 1942. The oceans. New York, Prentice-Hall. 1087 p.

Swanson, L. W. 1964. Aerial photography and photogrammetry in the Coast and Geodetic Survey. Photogrammetric Engineering, 30 (5): 699-726.

Tarkington, Raife G. 1966. The photographic process. In: Manual of photogrammetry, 3d ed., Menasha, George Banta Company p. 243-293.

Tyler, J. E. and W. H. Richardson. 1958. Nephelometer for volume scattering function in situ. Journal of the Optical Society of America 48 (5): 354-357.

Waldichuk, Michael. 1966. Currents from aerial photography in coastal pollution studies. Proceedings of the Third International Conference on Advances in Water Pollution Research, Munich. Baltimore, Port City Press, Inc. Vol. 3, p. 263-284.

Water Pollution Research Board. 1964. Coastal pollution. Report of the Director, Department of Scientific and Industrial Research, London. p. 136-142.

Wiegel, R. L. 1964. Oceanographical engineering. London, Prentice Hall International. 532 p.

Yost, E. F. and S. Wenderoth. 1967. Multispectral color aerial photography. Photogrammetric Engineering 33: 1020-1033.

The REMOTE SENSING CENTER was established by authority of the Board of Directors of the Texas A&M University System on February 27, 1968. The CENTER is a consortium of four colleges of the University; Agriculture, Engineering, Geosciences, and Science. This unique organization concentrates on the development and utilization of remote sensing techniques and technology for a broad range of applications to the betterment of mankind.